PERGAMON

International Journal of Heat and Mass Transfer 44 (2001) 2877–2887

International Journal of HEAT and MASS TRANSFER

www.elsevier.com/locate/ijhmt

A model for heat transfer in a pressurized circulating fluidized bed furnace

B.V. Reddy *, P. Basu [1]

Department of Mechanical Engineering, Dalhousie University, Halifax, Nova Scotia, Canada B3J 2X4

Received 7 April 2000; received in revised form 10 October 2000

Abstract

A mechanistic model based on cluster renewal approach is proposed to predict bed to wall heat transfer coefficient in a pressurized circulating fluidized bed (PCFB). The model takes into account the effect of pressure on cluster density, cluster thermal conductivity and particle convection heat transfer coefficient. The effect of pressure and bed temperature on bed to wall heat transfer coefficient is investigated. Published information on cluster velocity and bed hydrodynamics are used in the formulation of the model. The effect of cross-sectional average volumetric solids concentration on bed to wall heat transfer coefficient is also reported. The model predictions are validated against the experimental data obtained from a PCFB riser 52.4 mm in diameter and 2020 mm high. The unit is heated by electrical resistance heaters. The experimental results are reported for pressures up to 600 kPa and bed temperatures up to 650°C. The experimental data and model predictions are in reasonable agreement with each other. The model predictions are also validated with the data from the published literature, and a fair agreement is observed.

1. Introduction

Pressurized circulating fluidized bed (PCFB) technology is a recent extension of the fluidized bed technology family. This type of circulating fluidized bed operates at elevated pressures, but still maintains all the advantages of the circulating fluidized bed system. This technology is relatively new and is only at demonstration stage. An application of PCFB technology to the combined cycle power generation has opened up an attractive alternative due to its high overall efficiency, low pollution level, good heat transfer characteristics, compact furnace size and fuel flexibility. However, in order to fully comprehend the advantages of PCFBs, it is important to understand the effect of operating pressure on different design parameters. The bed to wall heat transfer is one such area where information is required. PCFB technology is in the demonstration stage. Limited information is available on hydrodynamics and heat transfer in pressurized circulating fluidized beds in the published literature. Shen et al. [1] experimentally investigated the effects of bed voidage and suspension density on heat transfer coefficient in a pressurized circulating fluidized bed unit. Wirth [2] and Molerus [3] conducted some experimental investigations in a 0.19 m diameter and 10 m high pilot scale PCFB unit. Recently Basu et al. [4] reported additional experimental data on the effect of system pressure and bed temperature on heat transfer coefficient in a PCFB unit. Basu et al. [5] reported results on the effect of temperature, suspension density and system pressure on heat transfer coefficient in a PCFB unit.

Basu et al. [5] proposed a mechanistic model by modifying their earlier model for CFB [6]. This model does not account for the effect of system pressure on parameters like fractional wall coverage by clusters (f), cluster solid fraction (c_{sf}) and on cluster and particle

* Corresponding author. Present address: Apt. 29, 2130, Saint-Laurent, Montreal, Quebec, Canada, H4M 1T2. Tel.: +1-514-340-4711; extn. 5912; fax: +1-514-340-4159.

E-mail addresses: bv_reddy@hotmail.com (B.V. Reddy), prabir.basu@dal.ca (P. Basu).

[1] Fax: +1-902-429-4867

0017-9310/01/$ - see front matter
PII: S0017-9310(00)00333-1

Nomenclature

A_r	Archimedes number, $d_p^3\rho_g(\rho_p-\rho_g)g\mu^{-2}$
C_1, C_2	correction factors
c	cross-sectional average volumetric solids concentration
c_g	specific heat of gas (J kg^{-1} K^{-1})
c_p, c_s	specific heat of particle, solid (J kg^{-1} K^{-1})
c_{pc}	specific heat of cluster (J kg^{-1} K^{-1})
c_{sf}	cluster solid fraction
d_i	inside diameter of the test section (m)
d_o	outer diameter of the test section (m)
d_p	mean particle size (μm)
e_c	emissivity of cluster
e_d	emissivity of dispersed phase
e_g	emissivity of gas
e_p	emissivity of bed material (particles)
e'_p	effective emissivity of particle cloud
e_w	emissivity of the wall
f	fraction of the wall covered by clusters
g	acceleration due to gravity (m s^{-2})
h	heat transfer coefficient from bed to the wall (W m^{-2} K^{-1})
h_c	cluster heat transfer coefficient (W m^{-2} K^{-1})
h_{cr}	radiation heat transfer coefficient between cluster and wall (W m^{-2} K^{-1})
h_{dr}	radiation heat transfer coefficient between the dispersed phase and wall (W m^{-2} K^{-1})
h_d	modified convection heat transfer coefficient between dispersed phase and the wall (W m^{-2} K^{-1})
h_{exp}	experimental bed to wall heat transfer coefficient (W m^{-2} K^{-1})
h_{rad}	radiation heat transfer coefficient (W m^{-2} K^{-1})
h_p	particle convection heat transfer coefficient (W m^{-2} K^{-1})
h_w	heat transfer coefficient due to conduction through gas layer (W m^{-2} K^{-1})
k_c	thermal conductivity of the cluster (W m^{-1} K^{-1})
k_t	thermal conductivity of the test section material (W m^{-1} K^{-1})
k_g	thermal conductivity of gas, gas film (W m^{-1} K^{-1})
k_p, k_s	thermal conductivity of the solid, particle (W m^{-1} K^{-1})
L_c	characteristic residence length of cluster at the wall (m)
P_r	Prandtl number
r_c	resistance due to transient heat conduction in the cluster (K W^{-1})
r_w	resistance due to gas film between the cluster and wall (K W^{-1})
t_c	residence time of cluster near the wall (s)
T_B	bed temperature (K)
T_w	wall temperature (K)
T_{wi}	test section inside wall temperature (K)
T_{wo}	test section outer wall temperature (K)
U_c	cluster velocity, (m s^{-1})
U_{mf}	minimum fluidization velocity (m s^{-1})
U_t	particle terminal velocity (m s^{-1})
Y	particle concentration in the dispersed phase, 0.001%

Greek symbols

ρ_c	density of the cluster (kg m^{-3})
ρ_{dis}	dispersed phase density (kg m^{-3})
ρ_g	gas density (kg m^{-3})
ρ_{go}	gas density at bed temperature under atmospheric pressure conditions (kg m^{-3})
ρ_p, ρ_s	particle density (kg m^{-3})
ρ_{sus}	cross-sectional average bed suspension density (kg m^{-3})
ε_c	volumetric void fraction of cluster
ε_{avg}	cross-section average bed voidage
δd_p	non-dimensional gas layer thickness between wall and cluster
σ	Stefan–Boltzman constant (W m^{-2} K^{-4})
μ	dynamic viscosity of gas (kg m^{-1} s^{-1})

convection heat transfer coefficients. The effect of gas gap thickness between cluster (δd_p) and heat transfer surface is also not accounted by Basu et al. [5]. Nag and Gupta [7] proposed a heat transfer model for PCFB but, the effect of gas density and cross-sectional average volumetric solids concentration on cluster and particle heat transfer coefficients are not accounted. Also, they did not use the available information on cluster velocity and residence time Noymer and Glicksman [8]. Nag and Gupta [7] used the correlation of Wen and Miller [9] to estimate gas convection heat transfer from bed to the heat transfer surface without accounting for the effect of system pressure and gas density on gas convection heat transfer coefficient.

The present work presents a mechanistic model to predict bed to wall heat transfer coefficient in a PCFB furnace. The model is based on the cluster renewal approach, and accounts for the effect of system pressure on different hydrodynamic parameters. Also, the recent information on cluster velocity and residence time are incorporated. Experiments were carried out to validate the model predictions of the effect of system pressure

and bed temperature on particle, gas and total heat transfer coefficients.

2. Model formulation

Agglomeration of solid particles into clusters or strands is a major characteristic feature of the circulating fluidized bed process. Fig. 1 shows the cluster renewal heat transfer mechanism in the core annulus structure in a PCFB riser column. The heat transfer model is based on the unsteady state heat conduction in strands or clusters traveling downwards along the heat transfer surface. The clusters are assumed to travel a certain distance, disintegrate and reform periodically in the annular layer of the riser. The influence of the downflowing clusters on heat transfer is predominant at the wall surface. When the clusters slide over the wall, an unsteady state heat conduction takes place from the clusters to the wall surface and the time averaged cluster heat transfer coefficient is given as [10]

$$h_c = \left(\frac{4k_c\rho_c c_{pc}}{\pi t_c}\right)^{0.5}. \tag{1}$$

The thermal conductivity of the cluster is calculated from the equation provided by Gelperin and Einstein [11] for packet heat transfer

$$\frac{k_c}{k_g} = 1 + \frac{M}{N}, \tag{2}$$

where $M$and $N$are given as follows:

$$M = (1-\varepsilon_c)\left(1 - \frac{k_g}{k_s}\right),$$

$$N = \frac{k_s}{k_g} + 0.28\varepsilon_c^{0.63(k_g/k_s)^{0.18}}$$

for particle diameter less than 0.5 mm and $k_s/k_g < 5000$.

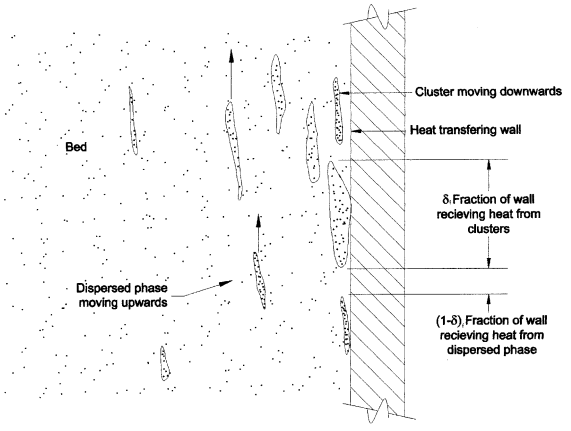

Fig. 1. Cluster renewal heat transfer mechanism.

The equation of Gelperin and Einstein [11] is modified to take into account the effect of pressure on thermal conductivity of cluster [12]

$$\frac{k_c}{k_g} = 1 + \frac{M}{N} + 0.1\rho_g c_g d_p U_{mf}. \tag{3}$$

The minimum fluidization velocity U_{mf} is predicted from the relation suggested by Chitester et al. [13] for higher pressures.

The specific heat and density of the clusters are estimated from the following relations. The effect of system pressure on the gas density and thereby on the cluster parameters are accounted from the relations

$$c_{pc} = (1-\varepsilon_c)c_s + \varepsilon_c c_g, \tag{4}$$

$$\rho_c = (1-\varepsilon_c)\rho_p + \varepsilon_c\rho_g, \tag{5}$$

where ε_c is cluster voidage and is calculated from the equation provided by Lints and Glicksman [14]. Since no information is available on PCFB hydrodynamics, this relation is extended to PCFB as a first approximation.

The relation between cluster solid fraction, c_{sf} and cross-section average volumetric solid concentration, c, in an atmospheric CFB is given by Lints and Glicksman [14]. As a first approximation the above relation is used at different system pressures.

Cluster solid fraction : $c_{sf} = 1.23c^{0.54}$

or

$$c_{sf} = 1.23(1-\varepsilon_{avg})^{0.54}, \tag{6}$$

where ε_{avg} is the cross-sectional bed average voidage. The cluster voidage ε_c is given by

$$\varepsilon_c = 1 - c_{sf}. \tag{7}$$

Clusters, formed in the riser, are often swept to the wall, owing to the low upward gas velocity in the wall region. The cluster travels downwards along the wall surface. It travels for a characteristic height L_c with an average velocity, U_c before disintegrating. No equation is available in the literature for estimation of t_c in high pressure beds. However, experimental measurements of Molerus and Wirth [15] show that the residence time decreases with system pressure. We can write the residence time of particles by correlating the data as [15]

$$\frac{t_p}{t_c} = 1.018 - 0.0166\left(\frac{P_p}{P_a}\right) - 0.0035\left(\frac{P_p}{P_a}\right)^2, \tag{8}$$

where t_p is the residence time at any system pressure and t_c is the residence time at atmospheric pressure conditions. The residence time at atmospheric pressure conditions in a circulating fluidized bed riser are presented by Wu et al. [16]. In the above equation P_p

represents system pressure (higher than atmospheric pressure) and P_a represents atmospheric pressure.

In addition to the resistance due to transient heat conduction in the cluster, a thin gas layer residing between the cluster and the wall will introduce another resistance to heat transfer from the cluster. The exact expression for transient conduction from a semi-infinite body to a surface with a series resistance is complicated. However, experimental measurements [17] have shown that the contact resistance and the transient conduction to the cluster of particles, act independently and they can be assumed to be in series with each other.

The expression for heat transfer coefficient due to conduction through this gas layer is

$$h_w = \frac{k_g}{\delta d_p}, \tag{9}$$

where δd_p is the thickness of the gas layer between the wall and cluster. Since, there is no evidence to suggest that δ would be influenced by pressure, the expression given by Lints and Glicksman [14] for atmospheric pressure circulating fluidized bed is used

$$\delta = 0.0282c^{-0.590}, \tag{10}$$

where c is the cross-section average volumetric solids concentration.

The particle convection heat transfer coefficient h_p, comprises heat conduction into the cluster and the conduction across the gas layer. So the heat transfer coefficient is given as

$$h_p = \left(\frac{1}{h_c} + \frac{1}{h_w}\right)^{-1}, \tag{11}$$

$$h_p = \left\{\left(\frac{\delta d_p}{k_g}\right) + \left(\frac{\pi}{4}\frac{t_c}{k_c \rho_c c_{pc}}\right)^{0.5}\right\}^{-1}. \tag{12}$$

The fraction of the wall, which is not covered by the clusters, i.e., $(1-f)$ receives heat from the gas–solid dilute dispersion flowing past it. The convection heat transfer from the dispersed medium to the wall is estimated by the modified equation of Wen and Miller [9], which was given by Basu et al. [5] as

$$h_d = \left(\frac{k_g}{d_p}\right)\left(\frac{c_p}{c_g}\right)\left(\frac{\rho_{dis}}{\rho_p}\right)^{0.3}\left(\frac{U_t^2}{g d_p}\right)^{0.21} P_r \left(\frac{\rho_g}{\rho_{go}}\right)^{0.2}. \tag{13}$$

The density of the dispersed phase ρ_{dis} is given by

$$\rho_{dis} = \rho_p Y + \rho_g (1 - Y), \tag{14}$$

where Y is the volumetric concentration of particles in the dispersed phase. The value of Y is recommended as 0.001% [5].

The fraction of the wall covered by clusters, f is given by Lints and Glicksman [14]

$$f = 3.5c^{0.37}, \quad f = 3.5(1 - \varepsilon_{avg})^{0.37}. \tag{15}$$

The convection heat transfer coefficient, combining the contributions of cluster as well as the dispersed phase is given as

$$h_{conv} = f h_p + (1 - f) h_d. \tag{16}$$

The radiation between the bed and the wall may be significant above 350°C. It may be assumed to act in parallel to the convection. This radiation heat exchange is similar to that between two parallel plates. The bed side plate is either cluster or dispersed phase. The cluster radiation component of the heat transfer coefficient is estimated from the equation given below.

$$h_{cr} = \left\{\frac{\sigma}{(\frac{1}{e_c} + \frac{1}{e_w} - 1)}\frac{(T_B^4 - T_w^4)}{(T_B - T_w)}\right\}, \tag{17}$$

where e_c is the emissivity of the cluster and e_w is the emissivity of the wall. The cluster emissivity, e_c is estimated from the following relation [18]:

$$e_c = 0.5(1 + e_p). \tag{18}$$

Many investigators in the literature suggested that the cooling of the cluster can be neglected and the cluster radiation can be treated as additive to cluster convection heat transfer coefficient for short length heat transfer surfaces. This approach may result some error in the cluster radiation heat transfer coefficient, but may be small. Further more, the fraction of wall covered by clusters is small. This is especially true in large industrial units where the cluster thickness (and hence the thermal capacity) is also high. So, unless the residence time on the wall is very long and clusters are thin the effect of cooling of clusters on the cluster radiation heat transfer can be neglected. In the PCFB literature not much is reported on cluster residence time near the wall. For longer heat transfer surfaces (1–2 m or more) the amount of error involved by using Eq. (17) can be estimated when the details on cluster residence time (hydrodynamics) are available.

The dispersed phase radiation heat transfer coefficient from bed to the wall is estimated from the following relation:

$$h_{dr} = \left\{\frac{\sigma}{(\frac{1}{e_d} + \frac{1}{e_w} - 1)}\frac{(T_B^4 - T_w^4)}{(T_B - T_w)}\right\}, \tag{19}$$

where e_d is the emissivity of the dispersed phase. For a very dilute medium, the effect of gas radiation can be taken into account by the following equation [19]:

$$e_d = (e_g + e'_p - e_g e'_p). \tag{20}$$

In the present case of air fluidized bed the gas emissivity, e_g is not a strong function of pressure. However, the situation may change, if the fluidizing gas contains non-luminous gases or if there is combustion in the bed.

The radiation from bed to the wall is made up of contributions of the cluster and the dispersed phase. So, the bed to wall radiation heat transfer coefficient is written as

$$h_{rad} = fh_{cr} + (1-f)h_{dr}. \quad (21)$$

The bed to wall heat transfer coefficient which is the combination of particle, dispersed phase convection heat transfer and radiation heat transfer is given as follows:

$$h = fh_p + (1-f)h_d + h_{rad}. \quad (22)$$

3. Results from the model

The predictions from the present model are discussed below. The variation of cluster thermal conductivity with system pressure for two different bed temperatures is shown in Fig. 2. The cluster thermal conductivity (k_c) is a strong function of bed temperature (gas thermal conductivity, k_g) and weak function of system pressure (gas density, ρ_g) as presented by Eq. (3). For the same pressure and cross-section average volume solids concentration (c), the cluster thermal conductivity increases very fast with bed temperature due to high gas thermal conductivity at higher bed temperatures. The cluster thermal conductivity increases moderately with the system pressure due to small rise in gas density for the same bed temperature and cross-section average volume solids concentration. The main mechanism for small rise in cluster thermal conductivity with pressure is the gas density which increases with pressure. The gas thermal conductivity increases with bed temperature, but it does not increase much with pressure. Fig. 2 clearly demonstrates this tendency. The cluster thermal conductivity increases with bed temperature due to the increase in gas thermal conductivity. Eq. 3 shows the combined effect of temperature, pressure and other parameters on the cluster thermal conductivity. The bed temperature plays a greater role than system pressure in enhancing the cluster thermal conductivity. The increase in cluster thermal conductivity contributes to higher cluster heat transfer coefficients.

From the work of Molerus and Wirth [15] we find that the particle residence time decreases with pressure. Also, we saw earlier that the cluster thermal conductivity increases at a fast rate with bed temperature and at slow rate with pressure. The combined effect of higher cluster conductivity and shorter residence time enhances the cluster heat transfer coefficient (Fig. 3). Also, higher system pressure and therefore gas density may have an effect on the thickness of the gas film between the cluster and the wall. Thus with higher system pressures, the thermal contact resistance between clusters and wall may decrease resulting in higher particle heat transfer coefficient. Fig. 3 shows the predicted particle heat transfer coefficient increases with system pressure as well as with temperature. The particle heat transfer coefficient increases at a high rate with bed temperature than with pressure. This is due to higher gas and cluster thermal conductivity.

The dispersed phase (gas) convection heat transfer coefficient (h_d) increases with system pressure (Fig. 4) as the gas density increases with system pressure. For a given system pressure an increase in bed temperature results in a higher gas thermal conductivity as the gas thermal conductivity increases with bed temperature. This increases the gas convection heat transfer coef-

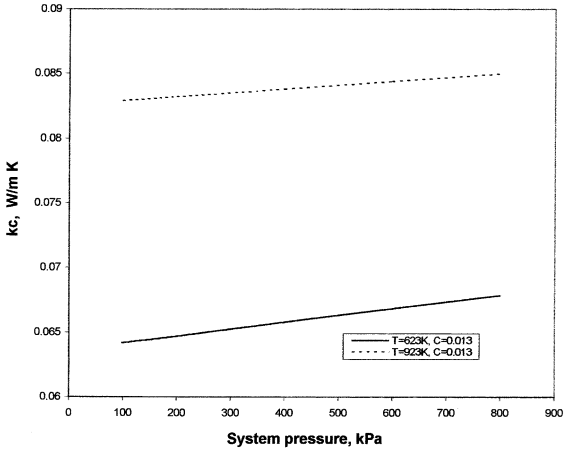

Fig. 2. Cluster thermal conductivity vs system pressure, $d_{p1} = 234$ μm.

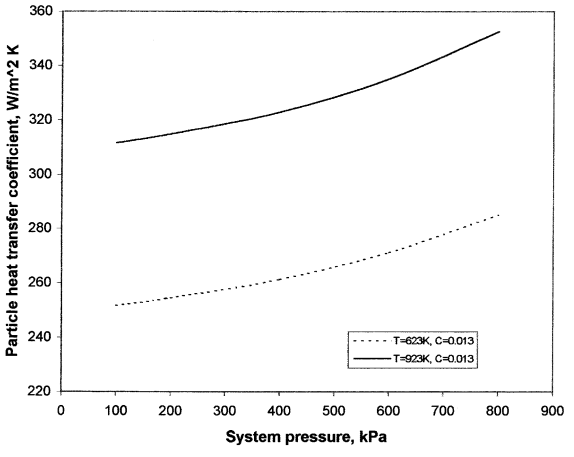

Fig. 3. Particle convective heat transfer coefficient (h_p) variation with system pressure, $d_{p1} = 234$ μm.

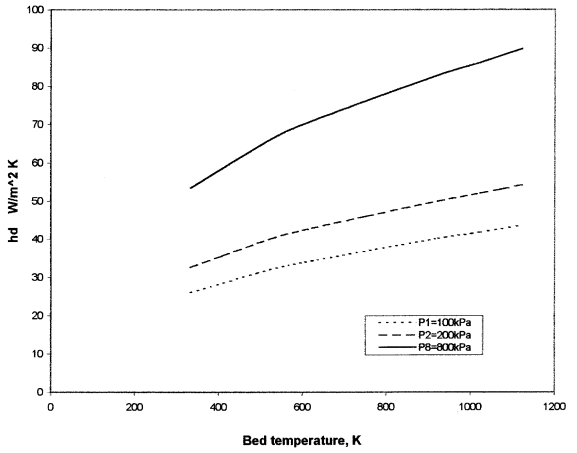

Fig. 4. Effect of bed temperature on dispersed phase (gas convective) heat transfer coefficient, $d_{p1} = 234$ μm, $c = 0.013$.

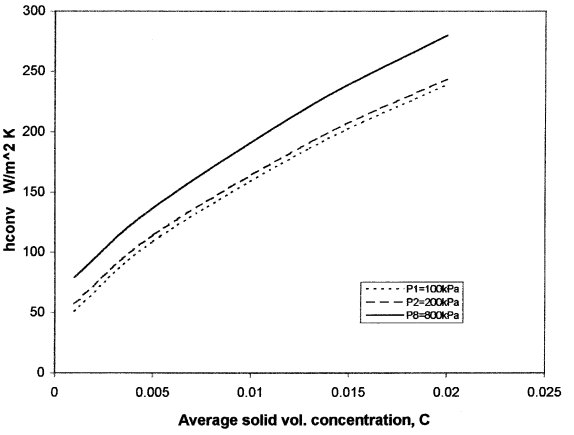

Fig. 6. Effect of average solid volume concentration on heat transfer coefficient (h_{conv}), $d_{p1} = 234$ μm, $T = 623$ K.

ficient. So, the dispersed phase convection heat transfer coefficient increases with pressure as well as with bed temperature. The rate of increase is higher with bed temperature than with system pressure.

The effect of system pressure on the convection component of the bed to wall heat transfer coefficient (h_{conv}) at different bed temperatures is shown in Fig. 5. Both components of the convection heat transfer coefficient (h_p, h_d) increases with bed temperature and system pressure. The rate of increase of h_{conv} with bed temperature is higher than system pressure. So, the convection heat transfer coefficient increases at a higher rate with bed temperature than with pressure.

The effect of cross-sectional average volumetric solids concentration (c) on bed to wall convection heat transfer coefficient (h_{conv}) is represented in Fig. 6. The bed to wall heat transfer coefficient increases with cross-sectional average volumetric solids concentration. This is due to the following reasons. The increase in cross-sectional average volumetric solids concentration increases the solid concentration within the cluster [14] and number of clusters near the wall. For other given conditions, the increase in cross-section average volume solids concentration (c), increases the cluster density, cluster thermal conductivity and cluster heat transfer coefficient. The presence of greater amount of solids in the cluster and the number of clusters near the wall enhances the particle heat transfer coefficient. The net result of the above factors is to increase particle convection heat transfer coefficient between the bed and the wall. Also, the dispersed phase convection heat transfer coefficient increases with bed temperature. The influence of all the above factors is to enhance the bed to wall heat transfer coefficient with cross-section average volumetric solids concentration.

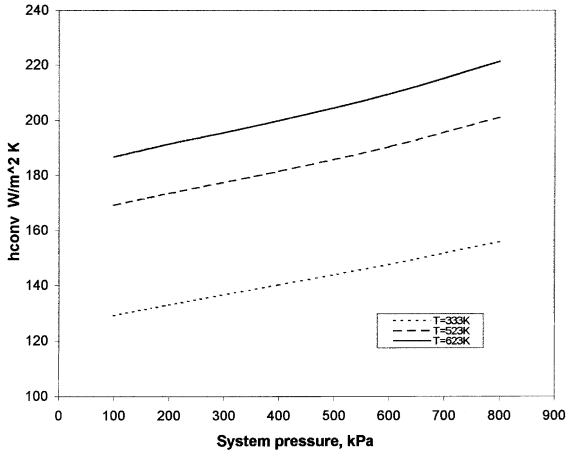

Fig. 5. Heat transfer coefficient (h_{conv}) variation with system pressure, $d_{p1} = 234$ μm, $c = 0.013$.

4. Experimental results

The experimental facility consists of a PCFB unit enclosed in an electrically heated chamber. Fig. 7 presents a schematic diagram of the PCFB unit. The riser is 52.4 mm in diameter (ID) and 2020 mm in height. The gas–solid suspension entrained from the riser column is separated in the cyclone separator attached to the riser. The separated solids are fed back into the main riser column through a loop seal. Additional details of the unit are reported elsewhere [4]. Most solids separated in the cyclone are returned to the bed through the standpipe and loop seal, a non-mechanical recycle control valve. Gas from the cyclone passes through the choking valve and then exited through the stack. The bed is enclosed in an electrically heated chamber, whose temperature can be controlled. Fig. 8 shows arrangement of

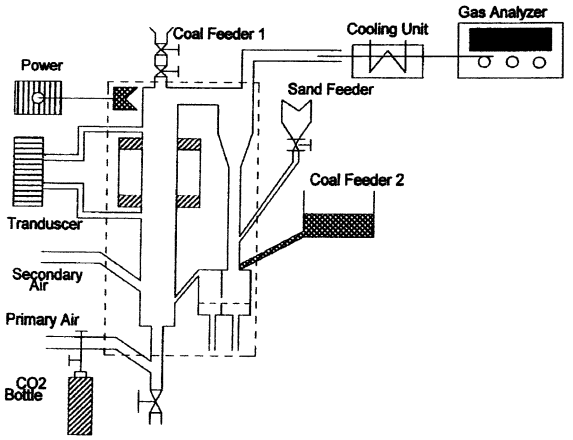

Fig. 7. Schematic diagram of the PCFB test rig.

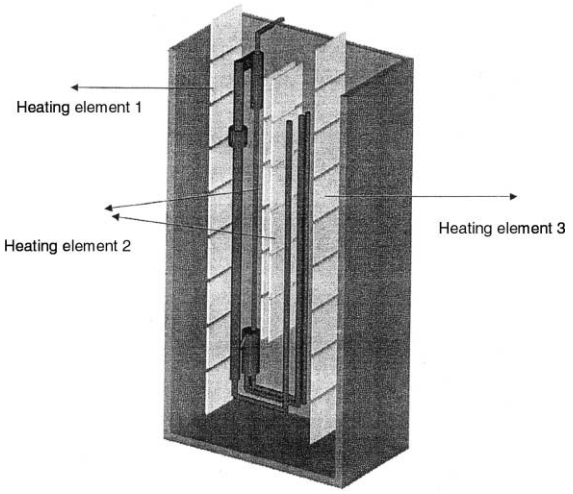

Fig. 8. Arrangement of heating elements in a PCFB test rig.

the heating elements. The furnace chamber operating temperature is pre-set before each test. Since the bed operates at high pressure and temperature, a special high strength and corrosion resistance material is selected to build it. The PCFB unit is made from inconel alloy 600, which has strength and resistance to corrosion. Associated lines including primary and secondary air lines are made of 316 stainless steel tubes. The cyclone and the loop seal are also made of inconel.

The bed is fluidized by air, which come from a high pressure air compressor delivering up to 700 kPa. The system pressure is changed by a choking valve arrangement, located down stream. The bed is operated in fast fluidized modes during the tests. The riser suspension density is calculated from the measured static pressure drops along the riser height. The measurement of static pressure drop in a PCFB is more

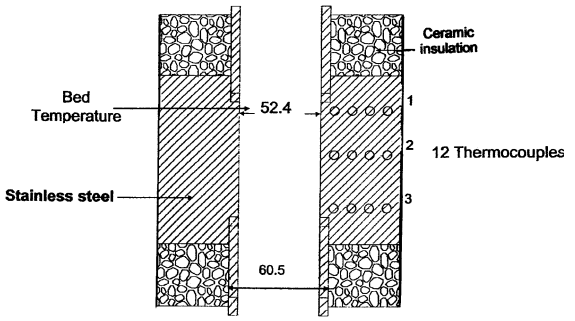

Fig. 9. Heat transfer test section with details.

difficult than that in an atmospheric CFB. A special metal filter with fine pores is installed in each pressure tap to prevent bed material plugging the pressure measurement line. Two instruments were chosen to measure the pressure drop. One is an inclined durblock solid plastic stationary gauge (range 0–4 in. of water). The other is an electronic pressure transducer, range 0–5 in. of water. To minimize the pressure difference across the wall of the transducer, the pressure transducer itself is mounted inside a vessel maintained at bed pressure.

A special technique was used to measure the bed to wall heat transfer coefficient. The heat transfer test section (Fig. 9) is made of stainless steel. It is located in the upper part of the bed. Its inside diameter is same as that of the bed column. The outer diameter of the test section is 140 mm and its height is 150 mm. Twelve K-type thermocouples are positioned at three levels with four in each level. These are positioned so as to give the radial temperature profile in the wall of the test section. Heat is transferred from the test section wall to the gas–solid suspension (bed) in the riser. Heat conducted through the wall of the test section is transferred to the bed. The wall to bed heat transfer coefficient is therefore estimated from energy balance neglecting heat losses

$$h_{\exp} = \left\{ \frac{2k_t}{d_i(T_{wi} - T_b)} \frac{(T_{wo} - T_{wi})}{\ln(d_o/d_i)} \right\}, \tag{23}$$

where k_t is the thermal conductivity of the heat transfer test section material. T_{wi} and T_{wo} are the inside and outside surface temperatures of the heat transfer test section, respectively. Here d_i is the inner diameter and d_o is the outer diameter of the test section. The bed temperature is measured by a thermocouple located near the test section. The unit is well insulated to prevent any axial heat loss. The experiments are conducted for two different mean sand particle sizes. The sand properties and the calculations are reported in [4]. The experiments are conducted for different system pressures (100–600 kPa) and bed temperatures (350–650°C).

5. Comparison of model predictions and experimental data

The details on the experimental conditions and calculations are reported elsewhere [4]. The predictions from the present model are compared with the experimental results for various operating conditions. The variation of bed to wall heat transfer coefficient (h) with system pressure for a particle size ($dp_1 = 234$ μm), bed temperature 350°C and for a particular suspension density ($\rho_{sus} = 21$ kg m^{-3}) is presented in Fig. 10. The heat transfer coefficient increases with system pressure. This is due to the increased particle and gas convection heat transfer with system pressure as discussed in the model results section. With system pressure the gas density increases, which results in higher cluster density. The cluster thermal conductivity increases moderately with system pressure due to increased gas density for the same bed temperature. Therefore, the cluster heat transfer coefficient increases with system pressure. The model also showed that the dispersed phase convection heat transfer coefficient increases with system pressure due to increased gas density. The net effect is that, the heat transfer coefficient increases with system pressure. Above experimental data were used in the model developed in Section 4. Eqs. (1)–(16) were used to predict heat transfer coefficient for the present experimental conditions. The operating temperature being low, radiation was neglected. Fig. 10 presents the comparison of experimental data and model predictions. The model predictions and experimental results are in reasonable agreement with each other. The deviations between model predictions and the experimental data can be attributed to the lack of information on the effect of system pressure on the parameters namely, cluster residence time (t_c), cluster characteristic length (L_c), cluster solid fraction (c_{sf}), fraction of the wall covered by cluster (f) and thickness of the gas gap layer between the wall and cluster (δd_p). At present, not much information is reported on PCFB riser hydrodynamics and on cluster characteristic length and residence time. Thus the model leaves enough room for modifications as the information on PCFB riser hydrodynamics comes in.

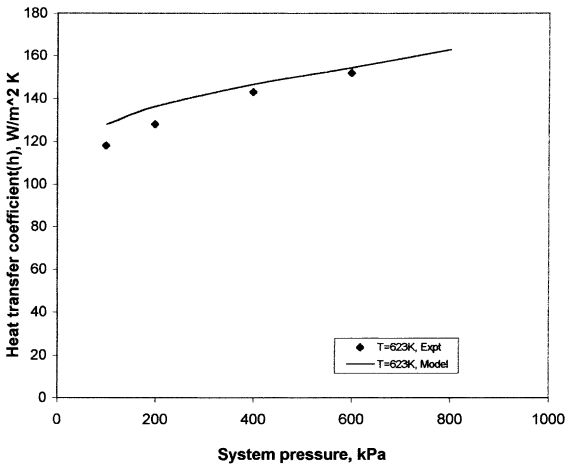

Fig. 10. Comparison of experimental data and model predictions, $d_{p1} = 234$ μm, $\rho_{sus} = 21$ kg m^{-3}.

The relative magnitudes of gas gap resistance between the cluster and wall (r_w) and resistance due to transient heat conduction in the cluster (r_c) are represented in Table 1. For low cross-sectional average volume solids concentration in the bed ($c = 0.005$, dilute bed) the wall gap resistance dominates than cluster resistance. As the cross-sectional average volume solids concentration increases ($c = 0.013$) cluster resistance dominates than wall gap resistance. For cross-section average volume solids concentration greater than 0.001 cluster resistance is more.

The experimental data for a particle size of 489 μm are compared with those predicted in Fig. 11. The experimental data and model predictions are in good, but not perfect agreement with each other. However, results for both particle sizes demonstrate the dominating effect of system pressure on heat transfer coefficient. The model shows a gentler in increase in heat transfer with pressure compared to those observed in the experiment.

Table 1
Relative magnitudes of resistance due to transient heat conduction in the cluster (r_c) and gas gap resistance between the cluster and the wall (r_w)

T_B (K)	r_c, $c = 0.005$	r_w, $c = 0.005$	r_c, $c = 0.013$	r_w, $c = 0.013$
$P = 100$ kPa, $d_p = 234$ μm				
623	0.00225	0.003136	0.00219	0.00178
923	0.001906	0.002352	0.00187	0.001338
1023	0.001826	0.002184	0.001795	0.001243
$P = 800$ kPa, $d_p = 234$ μm				
623	0.001758	0.003135	0.001724	0.001784
923	0.00152	0.002352	0.001498	0.001338
1023	0.00146	0.002184	0.001441	0.001243

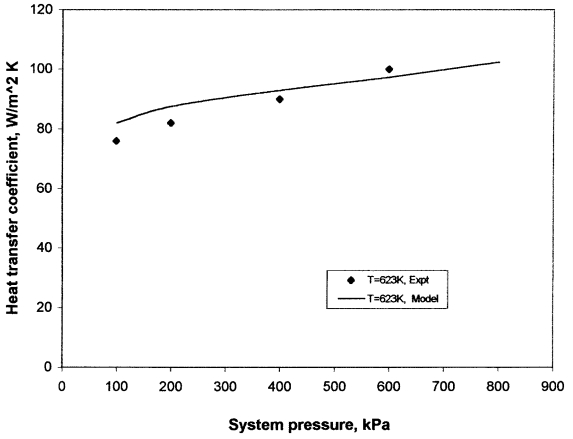

Fig. 11. Heat transfer coefficient (h) variation with system pressure, $d_{p2} = 489$ μm, $\rho_{sus} = 21$ kg m^{-3}.

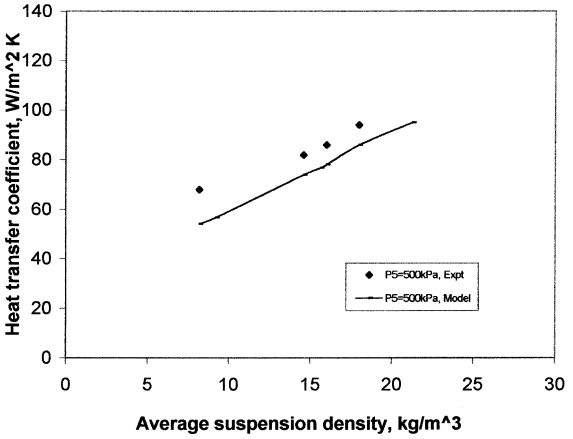

Fig. 12. Heat transfer coefficient (h) vs suspension density, $d_{p2} = 489$ μm, $T = 623$ K.

The effect of cross-sectional average bed suspension density on heat transfer coefficient for a system pressure of 500 kPa is shown in Fig. 12. The heat transfer coefficient increases with suspension density as observed in atmospheric pressure circulating fluidized beds. The increase in suspension density causes more number of clusters near the wall, higher cluster solid fraction and cluster heat transfer coefficient. The reasons for the rise has been explained in the model section also. It is interesting that unlike in Fig. 10, here the slopes of experimental data and those predicted from the model are similar although predicted values are lower than those measured. This suggests that which the present model accurately represents the effect of suspension density on heat transfer coefficient, but it does not accurately represent the effect of system pressure. This is particularly due to the lack of information on the effect of pressure on cluster residence time (t_c), cluster characteristic length

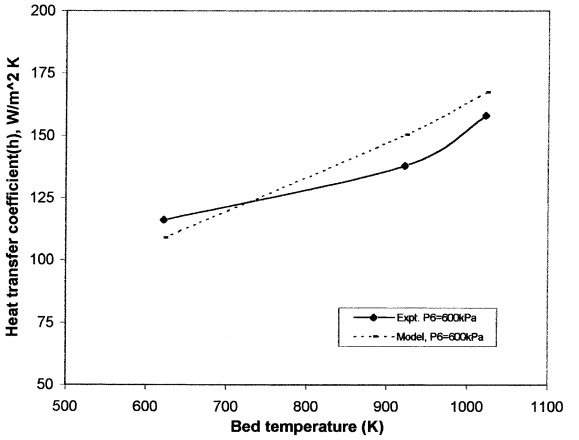

Fig. 13. Effect of bed temperature on heat transfer coefficient, model predictions and experimental data, $d_{p2} = 489$ μm, $\rho_{sus} = 21$ kg m^{-3}.

(L_c), cluster solid fraction (c_{sf}), fraction of the wall covered by cluster (f) and thickness of the gas gap layer between the wall and cluster (δd_p) in a pressurized circulating fluidized bed.

A comparison of model predictions and experimental results on the effect of bed temperature on heat transfer coefficient ($P = 600$ kPa) is demonstrated in Fig. 13. The heat transfer coefficient increases with bed temperature as generally observed in atmospheric circulating fluidized beds. The increase in bed temperature causes higher gas thermal conductivity and higher cluster thermal conductivity. The higher cluster thermal conductivity results in enhanced cluster and particle heat transfer coefficients. Also, the increased gas thermal conductivity increases dispersed phase convection heat transfer coefficient between the bed and wall. So the heat transfer coefficient increases at a higher rate with bed temperature for other given conditions. The effect of pressure on heat transfer coefficient may be more prominent in commercial boilers operating at low suspension densities may due to non-luminous radiation. In addition to the above reasons, the increase in bed temperature results in higher radiation heat transfer coefficient between bed and wall. The overall effect is that, the heat transfer coefficient increases at a fast rate with bed temperature. Although it was difficult to gather adequate experimental data points at a fixed pressure, the model and experimental predictions shows a reasonable agreement. The possible errors associated with the experimental data are presented below. Considering the uncertainties involved in the bed, surface temperatures and the heat flux, the possible errors associated with the experimental heat transfer coefficient are between ±4.1% and ±7.49%. The possible reasons

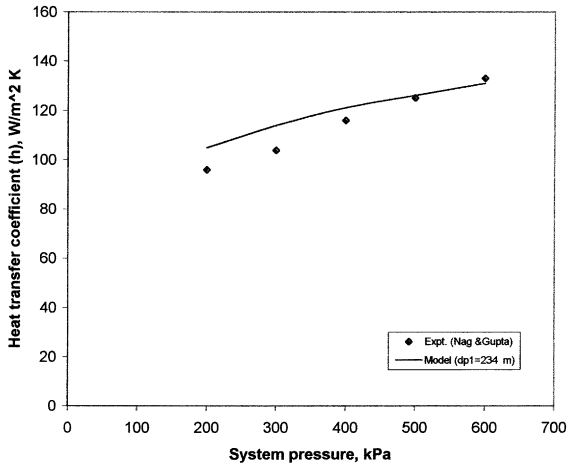

Fig. 14. Comparison of present model predictions with the experimental data of Nag and Gupta [7], $\rho_{sus} = 15$ kg m^{-3}, $d_p = 262$ μm.

for the deviation between experimental data and model predictions can be attributed to the lack of information available on certain hydrodynamic parameters. The hydrodynamic parameters are cluster residence time (t_c), cluster characteristic length (L_c), cluster solid fraction (c_{sf}), fraction of the wall covered by cluster (f) and thickness of the gas gap layer between the wall and cluster (δd_p). This results in the deviation between experimental data and model predictions.

Fig. 14 represents the comparison of model predictions ($d_p = 234$ μm) with experimental data of Nag and Gupta [7]. The heat transfer coefficient variation with system pressure is same in both the cases. The rate of increase of heat transfer coefficient with system pressure is little smaller compared to that of experimental data.

6. Conclusions

1. A model based on cluster renewal process can adequately explain the heat transfer behavior of a PCFB once the effect of pressure on thermophysical properties and the cluster residence time is accounted for.
2. The heat transfer coefficient increases with system pressure due to increased particle and dispersed phase convection heat transfer coefficients, as a result of the effect of pressure on the cluster thermal conductivity, capacity and residence time.
3. The increase in the suspension density results in higher cluster solid fraction and particle concentration near the wall, which results in higher heat transfer coefficients.
4. With increase in bed temperature, particle, gas (dispersed phase) convection and radiation heat transfer coefficients increases. Therefore, the heat transfer coefficient increases with bed temperature.
5. The model predictions and experimental data show the same trend and are in reasonable agreement with each other. The model predictions are also in agreement with experimental data of other investigators.

Acknowledgements

The authors acknowledge the financial support from Natural Science and Engineering Research Council of Canada. The authors also acknowledge Mrs. Sanja Boskovic for conducting the experiments.

References

[1] X. Shen, N. Zhou, Y. Xu, Experimental study on heat transfer in a pressurized circulating fluidized bed, in: P. Basu, M. Hasatani, M. Horio (Eds.), Circulating Fluidized Bed Technology, vol. 3, Pergamon Press, Oxford, 1991, pp. 451–456.
[2] K.E. Wirth, Heat transfer in circulating fluidized beds, Chem. Eng. Sci. 50 (1995) 2137–2151.
[3] O. Molerus, Arguments on heat transfer in gas fluidized beds, Chem. Eng. Sci. 48 (1993) 761–770.
[4] P. Basu, Leming Cheng, Sanja Boskovic, Heat transfer at high temperatures in a pressurized circulating fluidized bed, in: R.B. Reuther, Proceedings of the 15th International Fluidized Bed Combustion Conference, Paper no. FBC99-0033, vol. 1, 1999.
[5] P. Basu, Leming Cheng, Kefa Cen, Heat transfer in a pressurized circulating fluidized bed, Int. J. Heat Mass Transfer 39 (1996) 2711–2722.
[6] P. Basu, Heat transfer in high temperature fast fluidized beds, Chem. Eng. Sci. 45 (1990) 3123–3136.
[7] P.K. Nag, A.V.S.S.K.S. Gupta, A heat transfer model of pressurized circulating fluidized bed, in: J. Werther (Ed.), Circulating Fluidized Bed Technology, vol. 6, 1999, pp. 361–366.
[8] P.D. Noymer, L.R. Glicksman, Cluster motion and particle-convective heat transfer at the wall of a circulating fluidized bed, Int. J. Heat Mass Transfer 41 (1) (1998) 147–158.
[9] C.Y. Wen, E.N. Miller, Heat transfer in solid–gas transport lines, Industrial Eng. Chem. 53 (1961) 51–53.
[10] H.S. Mickley, D.F. Fairbanks, Mechanism of heat transfer to fluidized beds, Am. Institut. Chem. Eng. J. 1 (1955) 374–384.
[11] N.I. Gelperin, V.G. Einstein, Heat transfer in fluidized beds, in: J.F. Davidson, D. Harrison (Eds.), Fluidization, Academic Press, London, 1971, pp. 471–540.
[12] Y.G. Yates, Effects of temperature and pressure on gas–solid fluidization, Chem. Eng. Sci. 51 (1996) 167–205.

[13] D.C. Chitester, R.M. Kornosky, L.S. Fan, J.P. Danko, Characteristics of fluidization at high pressure, Chem. Eng. Sci. 39 (1984) 253–261.
[14] M.C. Lints, L.R. Glicksman, Parameters governing particle to wall heat transfer in a circulating fluidized bed, in: A.A. Avidan (Ed.), Circulating Fluidized Bed Technology, vol. 4, 1994, pp. 297–304.
[15] O. Molerus, K.-E. Wirth, Heat transfer in fluidized beds, Powder Technology Series, Chapman & Hall, London, 1997, pp. 12–14 (Chapter 2).
[16] R.L. Wu, J.R. Grace, C.J. Lim, A model for heat transfer in circulating fluidized beds, Chem. Eng. Sci. 45 (1990) 3389–3398.
[17] D. Gloski, L. Glicksman, N. Decker, Thermal resistance at a surface in contact with fluidized bed particles, Int. J. Heat Mass Transfer 27 (1984) 599–610.
[18] J.R. Grace, Fluidized bed heat transfer, in: G. Hestroni (Ed.), Hand Book of Multiphase Flow, McGraw-Hill, New York, Hemisphere,Washington, DC, 1982, pp. 9–70.
[19] B.A. Andersson, F. Johnsson, B. Leckner, Heat flow measurements in fluidized bed boilers, in: J.P. Mustonen, Proceedings of the Ninth International Conference on Fluidized Bed Combustion, ASME, New York, 1987, pp. 592–598.